Simulating the Use of Ancient Technology Works Using Advanced Virtual Reality Technologies

Konstantinos Moustakas, Dimitrios Tzovaras and Georgios Nikolakis

Simulating the Use of Ancient Technology Works Using Advanced Virtual Reality Technologies

Konstantinos Moustakas, Dimitrios Tzovaras and Georgios Nikolakis

This paper introduces a novel framework for the modeling and interactive simulation of ancient Greek technology works with the use of advanced virtual reality technologies. A novel algorithm is introduced for the realistic and efficient resolution of collisions that is based on an advanced collision detection approach that can also calculate in real-time the force that should be fed back to the user using a haptic device. Thus, the user is capable of manipulating the scene objects in the environment using haptic devices to simulate the sense of touch and stereoscopic imaging so as to be immersed in the virtual environment. Moreover, the virtual hand that simulates the user's hand is modeled using superquadrics so as to further increase the speed of the simulation and the fidelity of the force feedback. Extended evaluation of the system has been performed with visitors of the Science Center and Technology Museum of Thessaloniki.

1. Introduction

A recent trend in museums and exhibitions of Ancient Greek Technology is the use of advanced multimedia and virtual reality technologies for improving the educational potential of their exhibitions [1–3]. In [4] the authors utilize augmented reality technology to present an archaeological site. An attempt to visually enhance archaeological walkthroughs through the use of various visualization techniques is presented in [5]. A collaborative virtual environment system to navigate to a virtual historical city is presented in [6]. Authors of [7] present a variety of specialized hardware used in order to create interactive virtual spaces for museums or other cultural exhibitions. These include interfaces for navigation in large scale virtual spaces in museums utilizing new techniques in order to virtually enlarge and augment the exhibit surface.

The aforementioned examples show that museum exhibitions tend to be more and more interactive. Following this direction, the Thessaloniki Science Centre and Technology Museum, has created representations of ancient Greek technology in the form of small length video films in a PC, so that the visitor can comprehend exactly the operation of specific exhibits and observe their use in their initial operation environment. In a virtual representation enriched with narration, the visitor is provided with a very pleasant educational environment, where he/she can potentially achieve familiarization with the exhibit and in this manner obtain educational benefits.

Even if the acceptance of these applications by the museum visitors is considered to be high, there is a clear need for more realistic presentations that should be able to offer to the user the capability of interacting with the simulation, achieving in this way enhanced educational/pedagogical benefits.

A recent technology trend is the use of haptics for interactive simulations in a large variety of applications. Such applications include the access of information presented in 3D by blind and visually impaired users [8], engineers performing assembly planning [9] and students learning geometry [10] via the use of virtual reality environments (VEs).

However, these interactive applications involve several time-consuming processes that in most of the cases inhibit any attempt of real-time simulation. The most important of these processes are the collision detection [11,12,13], i.e. the identification of colliding parts of the simulated objects, and the haptic rendering [14][15], i.e. the calculation of the force that should be fed back to the user via a haptic device. Especially for the case of the simulation of ancient Greek technology works, where many parts of the mechanisms are in continuous collision with each other, there is need of efficient collision detection procedures so as to resolve all contacts in real time and to also provide the necessary force feedback to the user for haptic interaction with the virtual environment.

In the present paper we propose a novel framework for the simulation of ancient technology works using an efficient system for the detection of collisions that can also provide the appropriate force feedback in real-time.

Moreover, the virtual hand of the user that is used to handle scene objects is modeled using a set of analytical implicit surfaces [16] (superquadrics), so as to further increase the speed of the simulation and to provide a model that can be adapted to the user's hand. The general objective of the proposed application is the development of a framework for the simulation of Ancient Greek Technology works, with the use of advanced virtual reality technologies and direct user interaction. The main goal is to enhance the realistic simulation and demonstration of these technology works and to present their educational/pedagogical characteristics. The user is allowed to interact with the mechanisms in the virtual environment either by constructing or by using them via the proposed haptic interface.

The application aims to contribute to the development of a new perception of the modern era needs, by making reference to the technology evolution, efficiently demonstrating Ancient Greek Technology works, presenting their evolution in time and linking this evolution with corresponding individual and social needs.

The paper is organized as follows. In Section 2 the major aspects of the proposed framework are outlined. The collision detection and haptic rendering scheme are presented in Section 3. In Section 4, the functionalities of the authoring tool that is used for the design of the scenarios are described. Section 5 presents the evaluation scenarios and the experimental results, while Section 6 analyzes the evaluation procedure. Finally, the conclusions are drawn in Section 7.

2. System overview

Figure 1 illustrates the general architecture of the proposed framework. A simulation scenario is initially designed using the authoring tool and the available 3D content of the multimedia database. During the interaction with the user the core simulation unit takes as input the user's actions and the scenario.

Moreover, there are two types of software agents implemented in the context of the proposed framework, namely the geometry and the simulation agents [17]. The geometry agents apply constrains to the movement of the objects so as to enable the use of the ancient technology works in a natural way.

The simulation agents perform a high level interpretation of the user's actions and decide upon the next simulation steps. They enable or disable specific actions and control the assembling of components in order to construct a mechanism. The core simulation unit triggers each of the agents during each step of the interactive simulation.

In parallel, the collision detector checks for possible collision during each simulation step and whenever collision is detected the haptic rendering engine provides the appropriate force feedback to the user that is displayed using either the Phantom or the CyberGrasp haptic device. All these procedures result in the interactive simulation and assembly of ancient technology works.

► Figure 1: Architecture of the proposed framework.

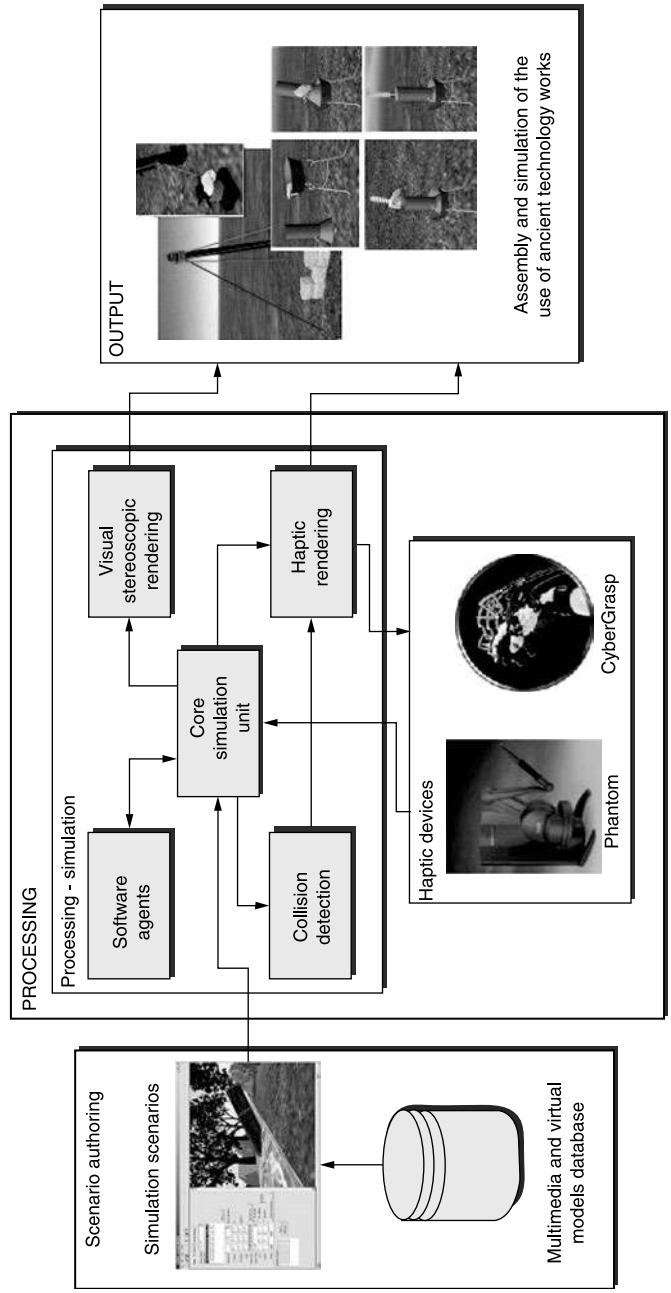

3. Collision detection and haptic rendering engine

The integrated collision detection and haptic rendering engine is based on a novel concept that is the modeling of the scene objects using analytical implicit surfaces (superquadrics). Initially, all objects are decomposed into rigid sub-objects that are subsequently modeled using the superquadrics so as the latter bound the geometry of each sub-object. Next an efficient

algorithm is developed to represent the underlying surface that uses only the analytical equation of the superquadric and the distances of the superquadric nodes to the mesh. These distances are stored into a 2D array that will be called *distance map* for the rest of the paper. Haptic rendering is performed utilizing the analytical formulae of the superquadric representation of the virtual hand.

3.1. Superquadric modeling

Superquadrics are a family of analytical implicit surfaces like superellipsoids, superparaboloids, superhyperboloids and supertoroids [16]. However, in the literature the term superquadric is usually used to describe superellipsoids, due to their high applicability. Superquadrics (superellipsoids) are described by the following implicit equation.

$$F(x,y,z)=\left(\left(\frac{x}{\alpha_1}\right)^{\frac{2}{\varepsilon_2}}+\left(\frac{y}{\alpha_2}\right)^{\frac{2}{\varepsilon_2}}\right)^{\frac{\varepsilon_2}{\varepsilon_1}}+\left(\frac{z}{\alpha_3}\right)^{\frac{2}{\varepsilon_1}}=1 \qquad (1)$$

Function *F* of Eqn (1) is commonly called inside-outside function, because for a 3D point *(x, y, z)*:

- If $F(x, y, z) > 1$, then *(x, y, z)* lies outside the surface.
- If $F(x, y, z) > 1$, then *(x, y, z)* lies inside or on the surface.

Three superquadric shapes are indicatively illustrated in Figure 2.

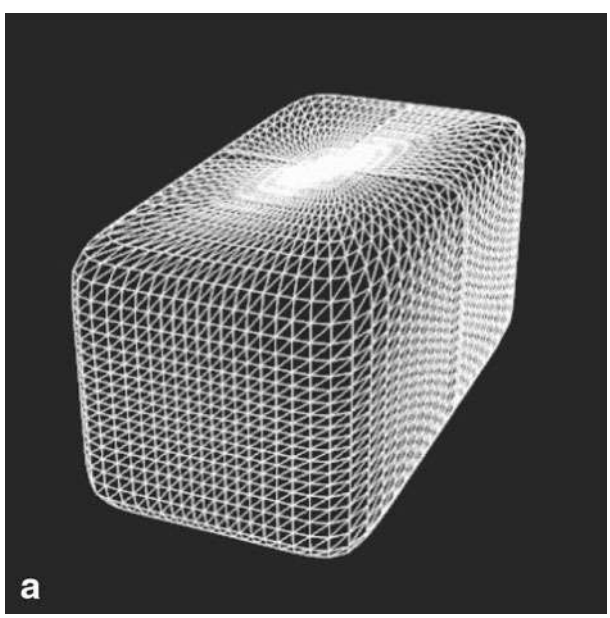

◀ Figure 2: Superquadrics with:
a: $\varepsilon_1 = 0.2, \varepsilon_2 = 0.2$.
b: $\varepsilon_1 = 0.2, \varepsilon_2 = 1.8$.
c: $\varepsilon_1 = 2.4, \varepsilon_2 = 3.2$.

► Figure 2. *(Continued)*

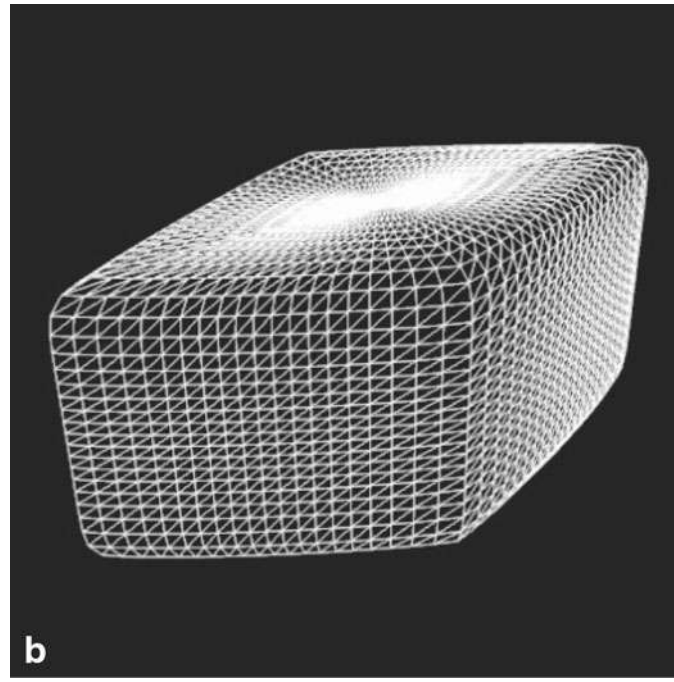

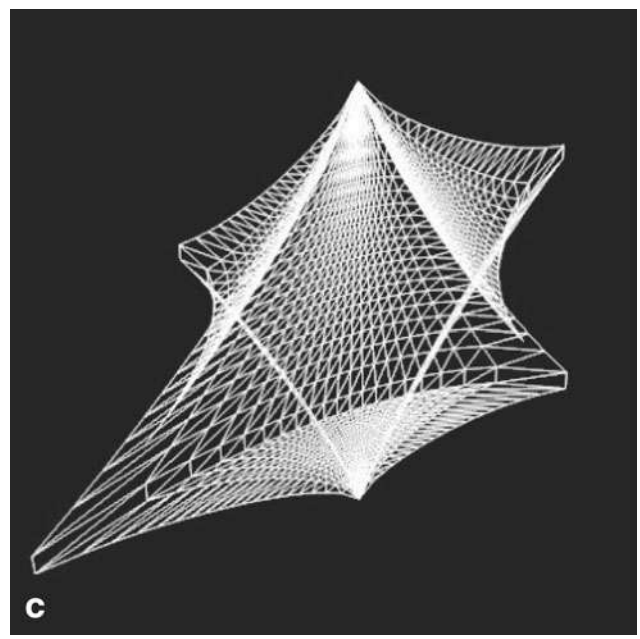

Deformation parameters, which correspond to tapering, bending, etc. [16], can be added to the implicit equation so as to produce a more flexible model. After the selection of the appropriate superquadric equation to model the 3D data, the problem of modeling the 3D object using a superquadric reduces to the least squares minimization of the nonlinear

inside-outside function *F(x, y, z)* with respect to several shape parameters. In particular,

$$F(x, y, z) = F(x, y, z; \alpha_1, \alpha_2, \alpha_3, \varepsilon_1, \varepsilon_2, \phi, \theta, \chi, t_x, t_y, t_z, K_x, K_y, k, \alpha) \quad (2)$$

where *(x, y, z)* is a point in the 3D space, $\alpha_1, \alpha_2, \alpha_3, \varepsilon_1, \varepsilon_2$, are the superquadric shape parameters, ϕ, θ, χ and t_x, t_y, t_z are the Euler angles and translation vector coefficients respectively, K_x and K_y are tapering deformation parameters and *k*, α the bending deformation parameters. The above parameters are determined so as to minimize the following mean square error.

$$MSE = \sum_{i=1}^{N} \sqrt{\alpha_1, \alpha_2, \alpha_3} \left(F(x_i, y_i, z_i) - 1 \right)^2 \quad (3)$$

where N is the number of points of the 3D object. The well-known Levenberg Marquardt method for nonlinear least squares minimization is used in the present paper in order to evaluate the shape parameters. Notice that for complex objects, proper division into rigid sub-objects is necessary for efficient superquadric approximation. Therefore, in the context of the proposed framework the visual saliency based algorithm [18][15] is used for decomposing the complex objects into their quasi-convex components.

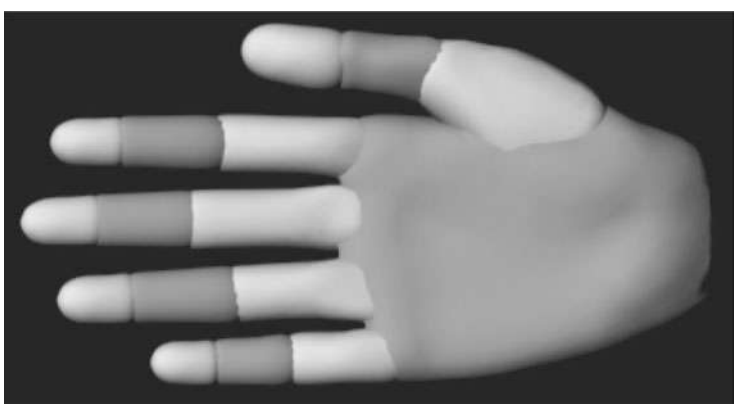

◀ Figure 3: Segmentation of the virtual hand.

Of particular interest is the superquadric approximation of the virtual hand. Figure 3 illustrates the segmentation of the virtual hand into its rigid components. Assuming that SQ_i represents the superquadric approximation of the ith element of the virtual hand, the superquadric representation of the whole virtual hand (VH) can be mathematically described as the union of all superquadrics:

$$VH = \sum_{i=1}^{16} SQ_i \quad (4)$$

In the proposed framework the virtual hand is totally configurable, by modifying the parameters of the superquadric, so as to be adaptable to the

user's hand. Since the calibration of the tracker and the haptic glove is of crucial importance for the simulation, the possibility of modifying the parameters of the virtual representation of the users hand is considered by the intermediate and also by the end users very promising.

3.2. Collision detection

The proposed superquadric collision detection procedure performs tests between the points of an object **A** and the superquadrics that comprise another object **B**. In order to refrain from these tests, when the objects are not close enough, bounding spheres are defined for each object, as well as for each superquadric. The smaller the number of SQ surfaces an object is decomposed to the faster the algorithm. In cases of fragmentation, which, however, are rare in practice, the algorithm can be easily combined with a hierarchical procedure for exploiting spatial coherency and minimizing the redundant operations. In the context of this work no more than two levels of bounding sphere hierarchies need to be used to provide satisfactory results.

Preprocessing

Initially, there is a need to calculate the distance between the generated superquadric and the original mesh so as to define the distance map. A dense mesh $r(\eta,\omega)$ is generated for the superquadric using its parametric equations.

$$r(\eta,\omega)=\begin{bmatrix}x\\y\\z\end{bmatrix}=\begin{bmatrix}\alpha_1\ \cos^{\varepsilon_1}\eta\cdot\cos^{\varepsilon_2}\omega\\ \alpha_2\ \cos^{\varepsilon_1}\eta\cdot\sin^{\varepsilon_2}\omega\\ \alpha_3\ \sin^{\varepsilon_1}\eta\end{bmatrix},\quad \forall\eta\in\left[-\frac{\pi}{2},\frac{\pi}{2}\right],\ \omega\in(-\pi,\pi) \qquad (5)$$

where η and ω are uniformly distributed in the specified intervals of Eqn (5). More precisely, η_d points are extracted for the η-space space and ω_d for the ω-space. After defining the superquadric mesh, the distance of each vertex from the original mesh is calculated. The distance map D(η,ω) is computed using Eqn (6),

$$D(\eta,\omega) = ICD\ (SQ, M) \qquad (6)$$

where *ICD* is the proximity evaluation function, which calculates the distance of every point (η, ω) of the superquadric SQ, alongside the normal direction at point (η, ω), from the mesh M and assigns the corresponding values to the distance map $D(\eta, \omega)$. The distance map is used in the sequel in order to allow the vertices of the second object involved in the collision to move freely inside the superquadric only within a specific distance from the superquadric, defined from $D(\eta, \omega)$.
A simple case of an object, the obtained superquadric and the calculated distanced map, is illustrated in Figure 4.

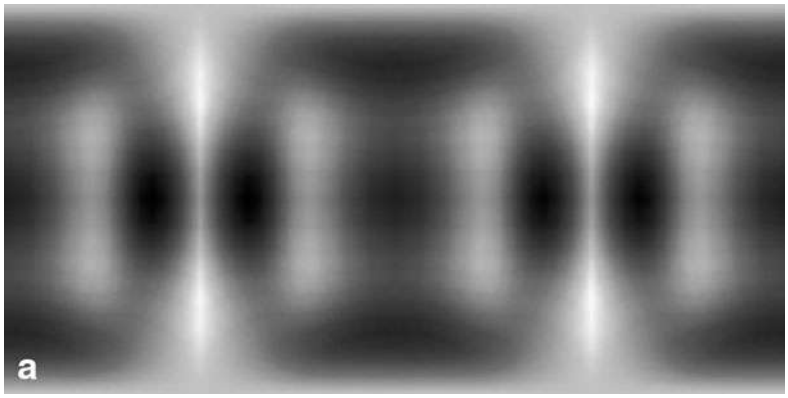

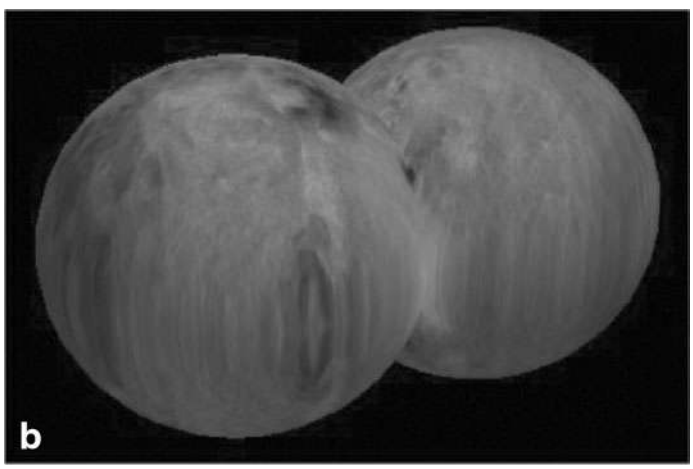

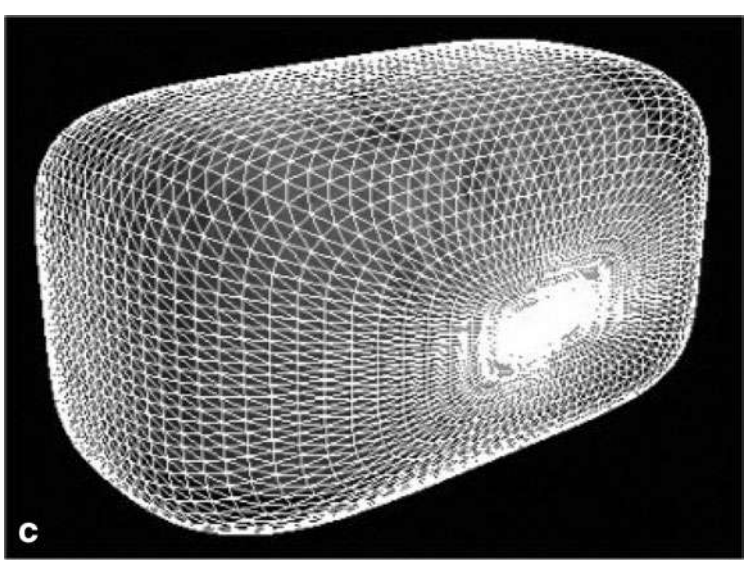

◀ Figure 4: a: An object composed of two spheres. b: its superquadric approximation. c: the resulting distance map, $\eta_d = 100$, $\omega_d = 200$. White corresponds to larger distance values.

Collision detection

At every time update of the simulation, the following collision detection procedure is executed. It should be mentioned that, in order to avoid collisions, each vertex $\mathbf{V}_B$ of object **B** possibly colliding with object **A**, which is modeled using superquadrics, has to be left to move freely without entering inside the original mesh **A** at each time instance, even if it lies inside the superquadric modeling object **A**. When checking for collision, not only the distance of $\mathbf{V}_B$ from the superquadric at the present frame has to be evaluated, but also the point of the superquadric, which corresponds to the minimum distance. An analytical estimation of the coordinates of this point is possible, but requires the solution of a *(4 × 4)* non-linear system of equations for each vertex [16]. This procedure is computationally complicated and unacceptable for real time applications. Therefore a fast multiresolutional search method is developed to find this minimum distance point. The main aspects of this method are described in the following for the 2D case of a superellipse, without loss of generality, in order to present more effectively important features in the figures.
Consider the superellipse of Figure 5a. Point **M** lies inside the curve and its minimum distance from the superellipse, as well as the minimum distance point $\mathbf{P}_M$ have to be evaluated. As illustrated in Figure 5a, for the minimum distance point $\mathbf{P}_M$, the normal vector to the surface passes through point **M**. The equation of the superellipse is:

$$\left(\frac{x}{a}\right)^{\frac{2}{\varepsilon}}+\left(\frac{y}{\beta}\right)^{\frac{2}{\varepsilon}}=1 \tag{7}$$

If $\varepsilon < 1$ (Figure 5a), point $\mathbf{P}_M$ corresponds to a larger value of angle θ ($\theta_{\mathbf{P}_M} > \theta_{\mathbf{M}}$), where θ is the variable of the parametric equation

$$r(\theta)=\begin{bmatrix}\alpha_1 \cos^{\varepsilon}(\theta)\\ \alpha_2 \sin^{\varepsilon}(\theta)\end{bmatrix},\quad -\pi\le\theta<\pi \tag{8}$$

Notice that $\frac{\pi}{4}<\theta_{\mathbf{P}_M}<\frac{\pi}{2}$. If $0<\theta_{\mathbf{P}_M}<\frac{\pi}{4}$ which is the case for point $\mathbf{P}_{M1}$ then $(\theta_{\mathbf{P}_{M1}} < \theta_{\mathbf{M}1})$. If $\varepsilon > 1$ the above inequalities become reversed as illustrated in Figure 5b. Assuming sets A and B, where

$$\begin{aligned}A&=\left\{k\frac{\pi}{2}<\theta<k\frac{\pi}{2}+\frac{\pi}{4}\right\}\\ B&=\left\{k\frac{\pi}{2}+\frac{\pi}{4}<\theta<(k+1)\frac{\pi}{2}\right\}\end{aligned},\quad k\in\mathbb{Z} \tag{9}$$

then

$$\begin{aligned}&\theta_{\mathbf{M}}>\theta_{\mathbf{P_M}},\ if\ \left(A\cap\{\varepsilon<1\}\right)\cup\left(B\cap\{\varepsilon>1\}\right)\\ &\theta_{\mathbf{M}}<\theta_{\mathbf{P_M}},\ if\ \left(B\cap\{\varepsilon<1\}\right)\cup\left(A\cap\{\varepsilon>1\}\right)\end{aligned} \tag{10}$$

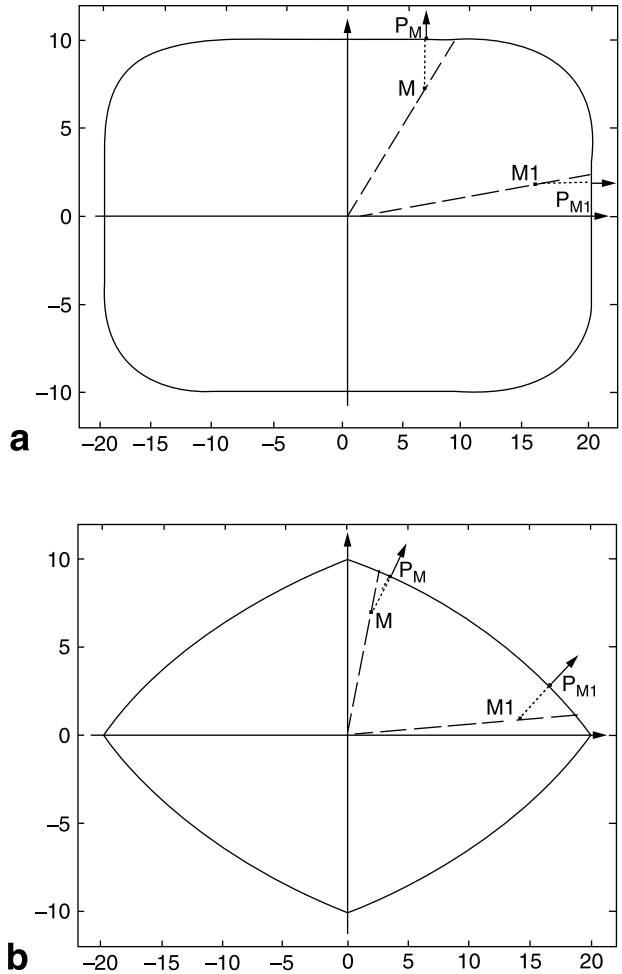

◀ Figure 5: Superellipses. a: $\varepsilon = 0.4$. b: $\varepsilon = 1.6$.

The above are simply extended for the case of the general 3D superquadric by simply replacing θ by η and ω. As a result, search directions are obtained for the two coordinate variables (η, ω) of the superquadric. Notice that despite the fact that the superquadric is a 3D surface in the 3D Euclidean space, it is only a 2D area in the non-Euclidean (curved) superquadric space. Thus, 2D search is performed in the area defined from points $(\eta_{\boldsymbol{M}}, \omega_{\boldsymbol{M}})$ and $(\eta_{\boldsymbol{M}} + \eta_r; \omega_{\boldsymbol{M}} + \omega_r)$, where η_r and ω_r are the search range variables as illustrated in Figure 6a, which can be positive or negative according to Eqn (10). Notice that the coordinate variables do not correspond to angle values of η and ω but to indices to their already performed quantization.

The search range is defined from the superquadric quantization density (η_d, ω_d) in the following way.

$$\eta_r = \omega_r = 2^N + 1 \tag{11}$$

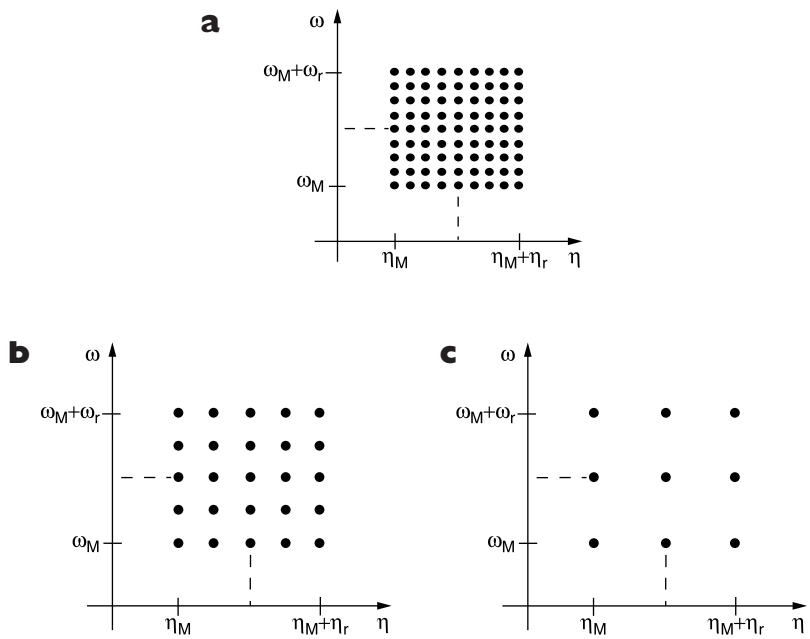

► Figure 6: Search pyramid for $N=3$, $\eta_r, \omega_r > 0$. a: Level 1. b: Level 0. c: Level 2.

where N is the integer part of

$$N = \max\left(\log_2 \frac{\eta_d}{16}, \log_2 \frac{\omega_d}{32} \right) \tag{12}$$

Figure 6 illustrates the levels of the created pyramid, which will be used in the 2D distance search method. The function I_S, to be maximized over the search region, is equal to the absolute internal product of the normalized normal vector to the superquadric surface at every point (η, ω) and the normalized line direction connecting points **M** and $\mathbf{P'}_M$.

$$I_s = \frac{1}{\left\| \mathbf{V}_{norm} \right\| \cdot \left\| \mathbf{L}_{dir} \right\|} \left| \mathbf{V}_{norm} \cdot \mathbf{L}_{dir} \right| \tag{13}$$

where $\mathbf{V}_{norm}$ is the spatial derivative vector of function F, which is defined in Eqn (1).

$$\begin{aligned} \mathbf{V}_{norm} &= \left[\frac{\partial F}{\partial x}, \frac{\partial F}{\partial y}, \frac{\partial F}{\partial z} \right]^T \\ \mathbf{L}_{dir} &= \left[X_{\mathbf{P'}_M} - X_{\mathbf{M}}, Y_{\mathbf{P'}_M} - Y_{\mathbf{M}}, Z_{\mathbf{P'}_M} - Z_{\mathbf{M}} \right]^T \end{aligned} \tag{14}$$

Function I_S is maximized for point $\mathbf{P}_M$ (as shown in Figure 5 a), since in this case the vectors $\mathbf{V}_{norm}$ and $\mathbf{L}_{dir}$ are approximately collinear. As noted earlier, the hierarchical search procedure is applied to find the point $\mathbf{P}_M$ that maximizes I_S: Initially, the function I_S is evaluated for the points of the top level N. Next, I_S is

evaluated at level *N-1* for the neighbors of the point, which produce the higher I_S value at level *N*. The procedure is repeated until the bottom level is reached and point $\mathbf{P}_M$ is found. The hierarchical search method requires $8N + 1$ evaluations of function I_S instead of $(2N + 1)\times(2N + 1)$ of the exhaustive search. After locating point $\mathbf{P}_M$, the distance D_{SQ} of this point from the original mesh is available from the distance map generated during the preprocessing stage. If the distance of point **M** from point $\mathbf{P}_M$ is higher than D_{SQ}, collision is detected.

3.3. Haptic rendering

In the context of the proposed framework a simple and efficient haptic rendering scheme has been developed that utilizes the superquadric representation of the virtual hand to rapidly estimate the force feedback. Consider that point **P** is detected to lie inside a segment of the virtual hand (Figure 7). Let also S^p_{SQ} represent the distance of point **P** from the

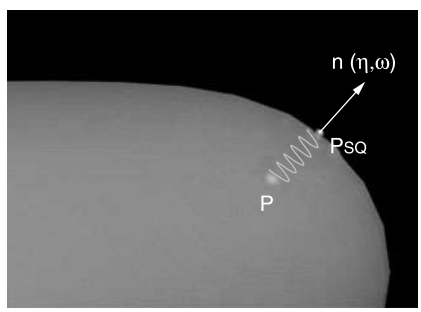

◀ Figure 7: Force feedback evaluation.

superquadric, which corresponds to point $\boldsymbol{P}_{SQ}$ on the superquadric surface, i.e. $\boldsymbol{P}_{SQ}$ is the projection of **P** onto the superquadric. The amplitude of the force fed onto the haptic devices is obtained using a simple spring model as illustrated in Figure 7. In particular:

$$\|\mathbf{F}\| = k \cdot S^p_{SQ} \tag{15}$$

where *k* is the stiffness of the spring. The rest length of the spring is set to zero so that it tends to bring point **P** onto the superquadric surface. The direction of the force feedback is evaluated in most state-of-the-art approaches using the triangulated mesh of the objects. In particular, it is set to be perpendicular to the triangle, for which collision has been detected. This approach is not only computationally intensive, but also results in non-realistic non-continuous forces at the surface element boundaries. In the present framework the already obtained superquadric approximation is used in order to rapidly evaluate the force direction. More precisely, the direction of the force feedback is set to be perpendicular to the superquadric surface at point $\boldsymbol{P}_{SQ}$. In particular using the parametric representation of the

superquadric, Eqn (5), the normal vector is defined at point $\boldsymbol{r}(\eta,\omega)$ as the cross product of the tangent vectors along the coordinate curves [8].

$$\begin{aligned}\mathbf{n}(\eta,\omega) &= \mathbf{t}_{\eta}(\eta,\omega) \times \mathbf{t}_{\omega}(\eta,\omega) \\ &= s(\eta,\omega)\left[\frac{1}{a_1}\cos^{2-\varepsilon_1}\eta\cdot\cos^{2-\varepsilon_2}\omega,\ \frac{1}{a_2}\cos^{2-\varepsilon_1}\eta\cdot\sin^{2-\varepsilon_2}\omega,\ \frac{1}{a_3}\sin^{2-\varepsilon_1}\eta\right]^T\end{aligned} \tag{16}$$

where

$$s(\eta,\omega) = -a_1a_2a_3\varepsilon_1\varepsilon_2\ \sin^{\varepsilon_1-1}\eta\cdot\cos^{2-\varepsilon_1-1}\eta\cdot\sin^{\varepsilon_2-1}\omega\cdot\cos^{\varepsilon_2-1}\omega \tag{17}$$

If several points lie inside the superquadric, the force fed to the haptic device is the average force of all penetrating points. Thus, the force feedback is obtained using Eqn (18).

$$\mathbf{F} = \frac{k}{N}\sum_{i=1}^{N} s_{SQ}^{P_i}\frac{\mathbf{n}(\eta_i,\omega_i)}{\left\|\mathbf{n}(\eta_i,\omega_i)\right\|} \tag{18}$$

The CyberGrasp haptic device, which is used to test the proposed methods, provides feedback only along the perpendicular direction to the user's fingers as illustrated in Figure 8.

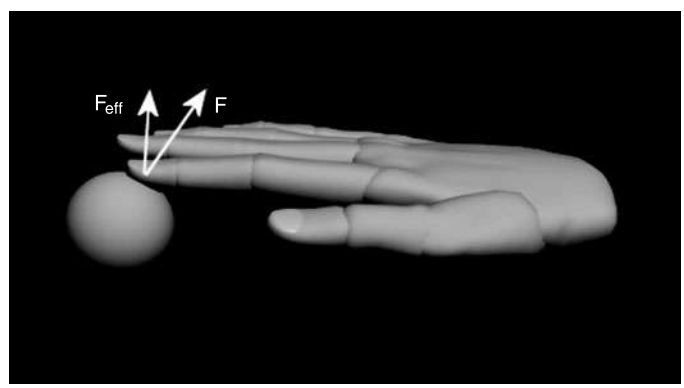

► Figure 8: Force feedback for the CyberGrasp.

Thus, if $\mathbf{n}_f$ is the perpendicular direction to a finger, the effective force, $\mathbf{F}_{eff}$, fed onto the haptic device is:

$$\mathbf{F}_{eff} = \left\langle \mathbf{F}, \mathbf{n}_f \right\rangle \cdot \mathbf{n}_f \tag{19}$$

4. THE AUTHORING TOOL

In order to support the extensibility of the proposed system an authoring tool was created that provides a user friendly environment to the expert user for manipulating all the necessary data in order to create an educational scenario. A screenshot of the developed authoring tool is illustrated in Figure 9. This is a very powerful and extensible authoring tool

for the creation of ancient Greek technology presentation scenarios to be simulated by the application. The tool provides: (a) functionalities for the composition of 3D simulations, (b) capability of connecting with the VR haptic devices (c) capability of parameterizing the intelligent software agents that simulate the functionality of parts (or the whole) of Ancient Greek mechanisms, (d) capability of composing, processing and storing scenarios, (e) integration of various scenarios and the possibility to save in a new scenario and (f) capability of modifying haptic parameters of the objects. The authoring tool allows the user to create and modify educational scenarios that can be imported in the platform. The expected complexity of the scenario files, lead to the adoption of the X3D standard as the scenario format, in order to be able to create more realistic applications. Information that cannot be supported directly from the X3D format is stored as a meta tag of the X3D scenario file. The tool allows the user to select virtual reality agents, associate them with objects in the scene, insert and modify their parameters and provide constrains to them. Each scenario may contain one or more steps. The objects may have different characteristics and associations in each step according to the scenario needs. The author can control the flow of a scenario using simple arithmetic rules (i.e. <, >, =) in order to trigger the next step in the scenario depending on the actions of the user.

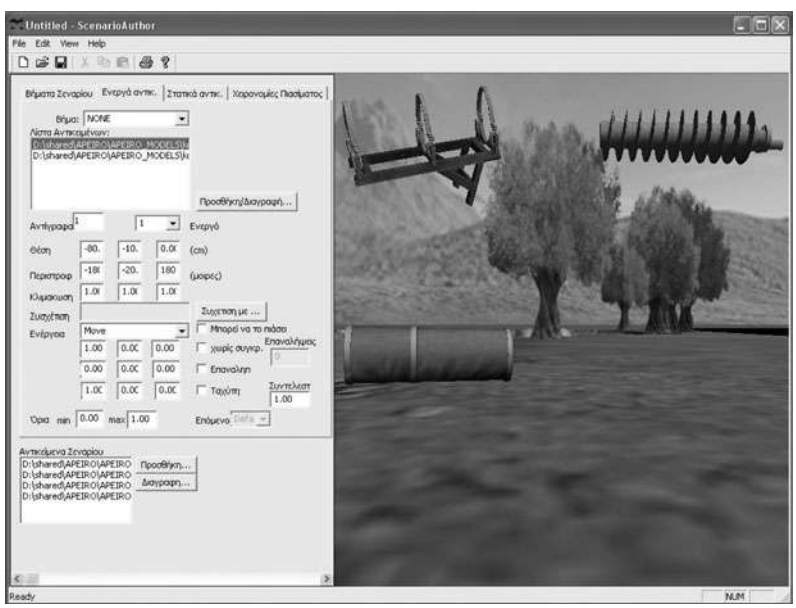

◀ Figure 9: The simulation scenario authoring tool.

5. Experimantal results

Several simulations were performed to evaluate the proposed framework. The general simulation scenario consists of an ancient Greek village, where several ancient Greek technology mechanisms are distributed in specific places as illustrated in Figure 10. The user is able to both use and assemble

the demonstrated mechanisms from their spare parts using whether the CyberGrasp or the Phantom haptic devices. The user can select the scenario by clicking on a sign with the mouse or by touching the sign with his/her index finger. In the following, some of the scenarios are indicatively presented.

► Figure 10: The ancient village.

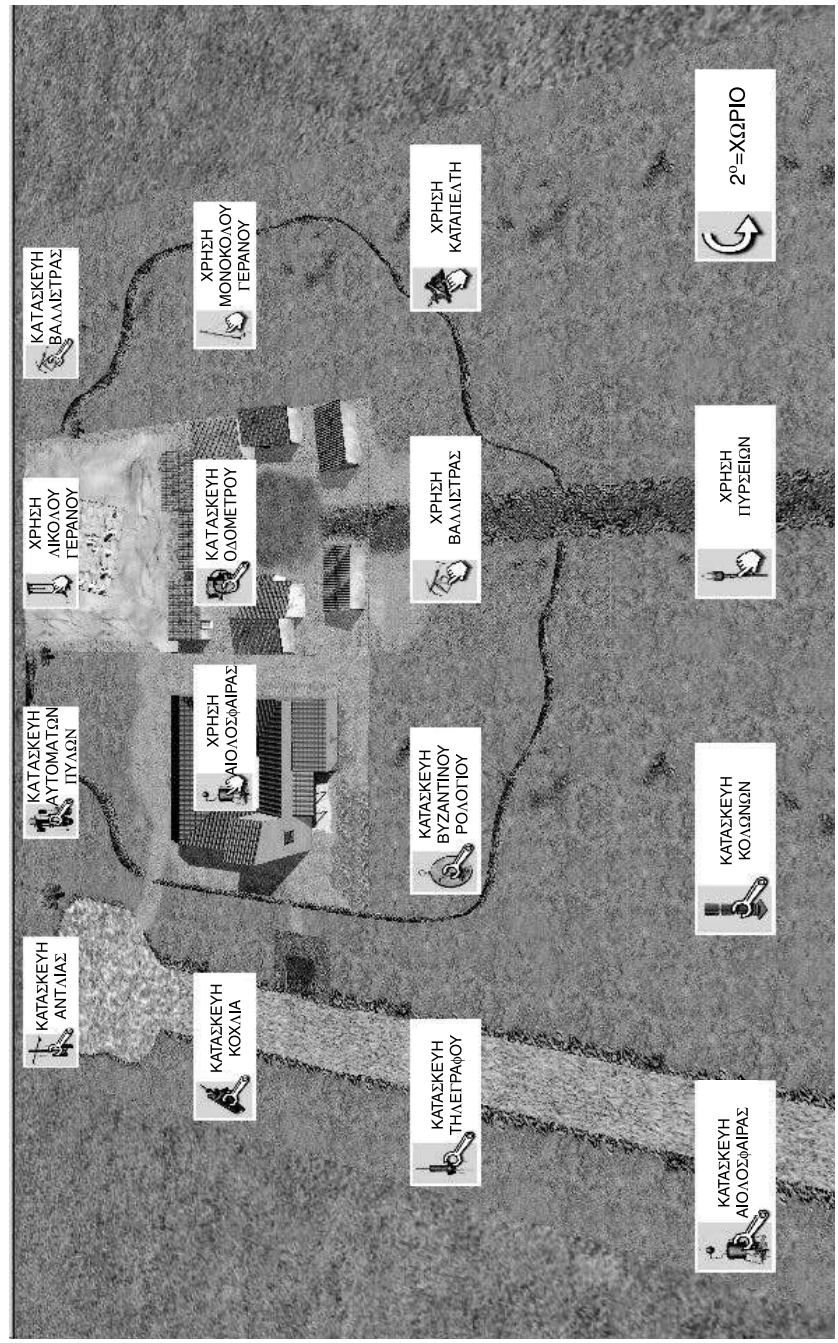

5.1. Pumps

Two pumps are simulated using the application; namely the Archimedes screw pump and the Ktisivios pump. The Archimedes screw pump is shown in Figure 11 a. The user can either assembly or use the pump. In the

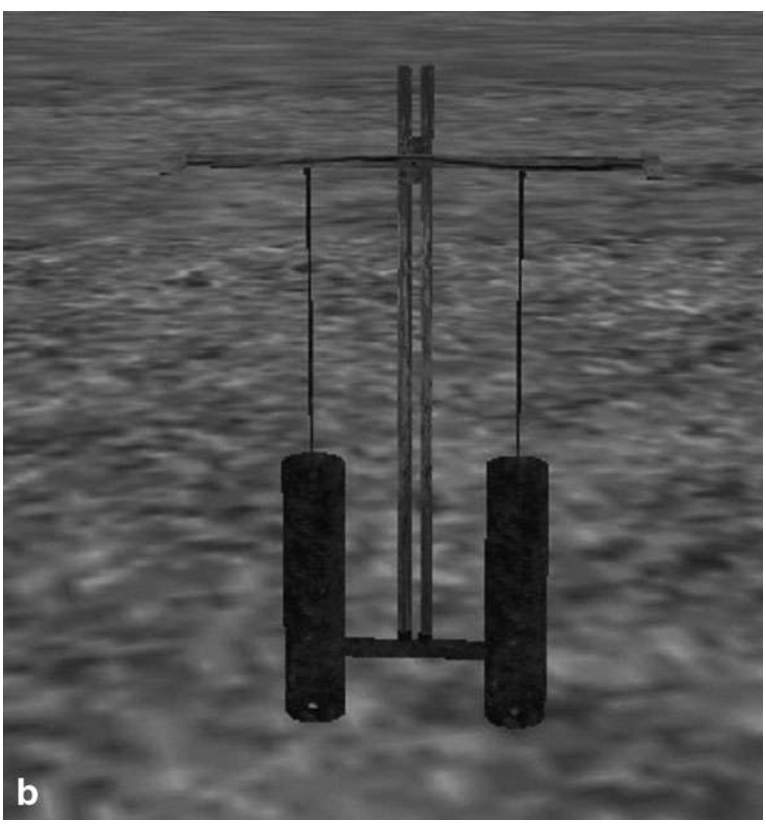

◀ Figure 11: a: Archimedes screw-pump. b: Ktisivios pump.

latter scenario the user has to grasp the handle of the pump and rotate it along the axis in order to pump water from the river. The level of the water in the pump depends on the angular speed of the handle. When the speed exceeds an upper limit, water flows off the pump. The assembly scenario is a simple scenario where the users can grasp the inner part of the pump and place it inside the outer cylinder in order to complete the task. This is used as a first step to get the user acquired with the application.
The Ktisivios pump is shown in Figure 11 b. The assembly scenario is a simple scenario where the user has to put the inner parts of the pump inside the main body of the pump and then add the handle on the top, while in the simulation scenario the user has to move the handle up and down.

5.2. Cranes

The single pulley crane is shown in Figure 12 a. The user has to pull a rock in order to construct a wall, using the single pulley crane. To achieve this, the user must grasp the handle that lies on the floor next to the crane and rotate it. In the right bottom corner the user can see a detail of the mechanism. The double pulley crane is shown in Figure 12 b. The user has to pull a rock in order to construct a column, using the double pulley crane. The functionality of this scenario is similar to the single pulley crane. In the right bottom corner the user can see a magnified part of the mechanism.

5.3. War machines

The catapult is shown in Figure 13 a. The user must grasp and pull the handle on the right side of the catapult in order to wind up the catapult mechanism. Then the user can throw a rock to destroy the wall by pulling the security trigger. The crossbow is shown in Figure 13 b. The user has to wind up the crossbow mechanism and then throw an arrow by pulling the security trigger.

5.4. Other ancient works

The sphere of Aiolos is shown in Figure 14 a. In the simulation scenario the user lights a fire on the under the mechanism and the sphere starts rotating. The Odometer is shown in Figure 14 b. The user can either construct or use the odometer. The side of the odometer is transparent so that the user can view how it works.

5.5. Quantitative results

The proposed framework for the simulation of ancient Greek technology works was tested in the context of the performed scenarios and was compared to other popular state-of-the-art approaches for collision detection and haptic rendering [11,12,14].

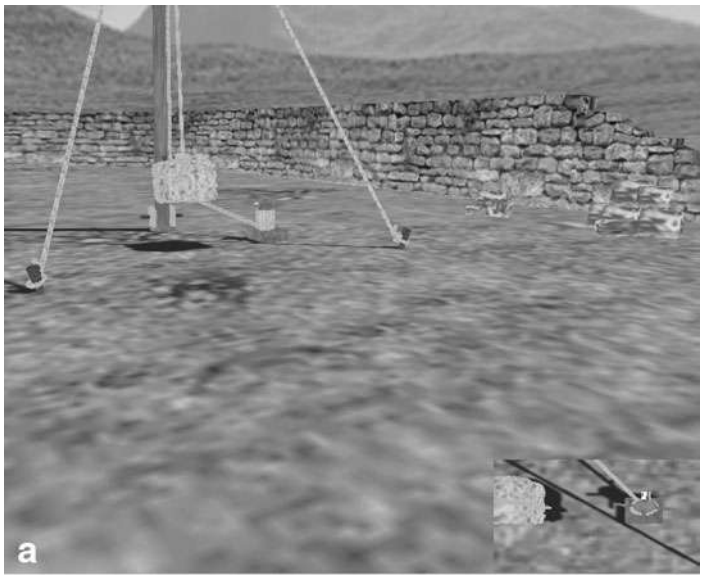

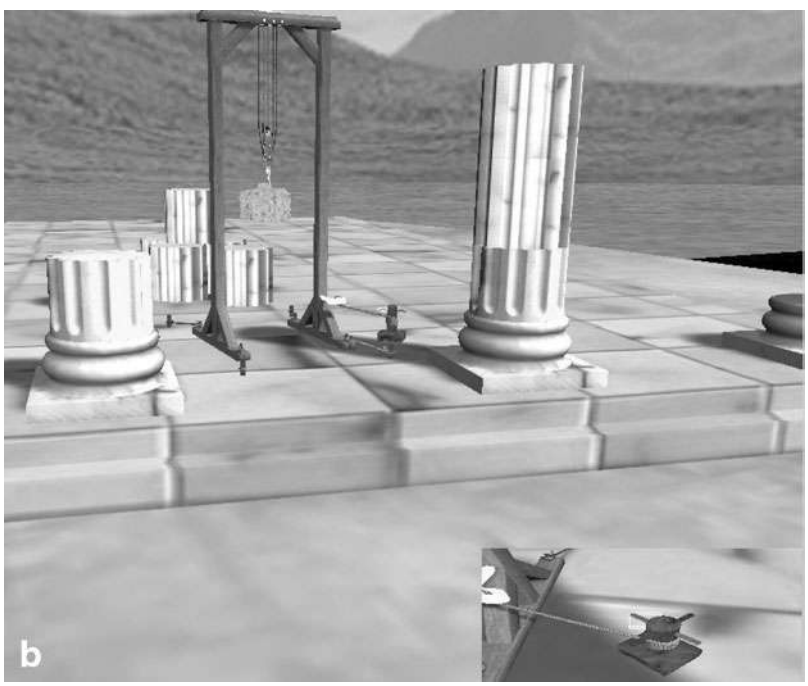

◀ Figure 12: a: Single pulley crane. b: Double pulley crane.

Figure 15 a illustrates the percentage of the time needed to perform collision detection with the proposed method, using as reference the method described in [11]. The difference in efficiency is obvious and haptic rendering update rate of 1kHz can be achieved even for large and detailed virtual environments. While collision does not occur and the algorithms perform tests only for the bounding volumes, the two methods do not

► Figure 13: a: Catapult. b: Crossbow.

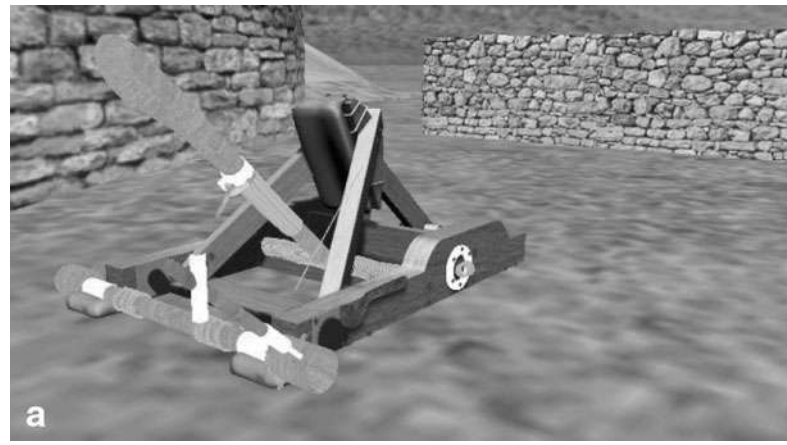

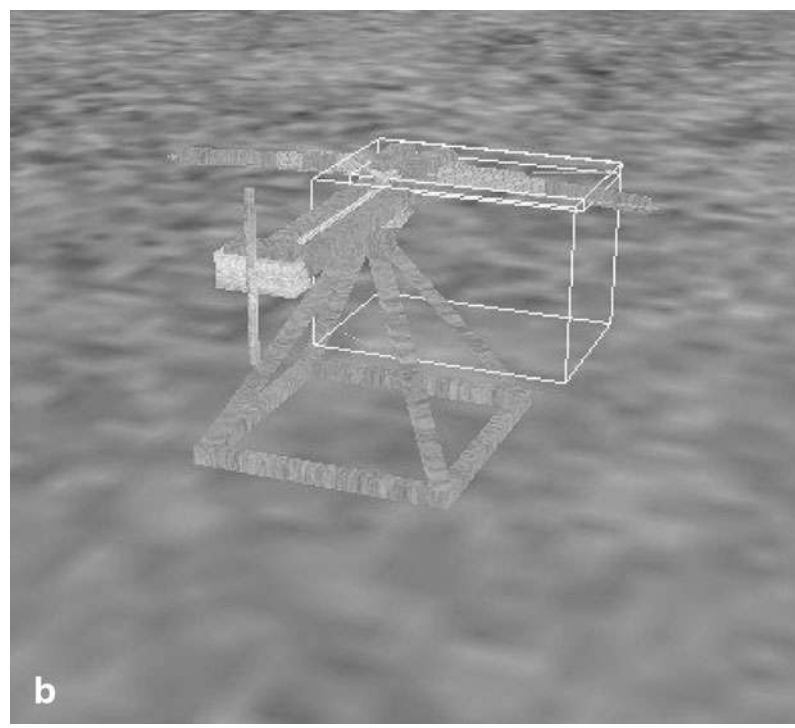

differ significantly, which is the case for the first few time-steps. When the user approaches and grasps the scene objects the proposed method performs much faster than the mesh based approach.

Equivalent gain in speed can be obtained using the distance field method [13]. Despite their efficiency, the distance field methods are not used excessively for collision detection. The major reason is their huge memory requirements. Adaptively sampled distance fields [19] have been presented in

◀ Figure 14: a: Sphere of Aiolos. b: The odometer.

the past in order to decrease the cost in memory. However, the memory requirements remain extremely high and can reach the size of many hundreds of MegaBytes for relatively complex environments, while the proposed method requires only the storage of the parameters of each superquadric and the associated distance map. An illustration of the memory requirements of the Distance field, the adaptive distance and the proposed scheme is illustrated in Figure 15 b.

Moreover, as illustrated in Figure 16, the force feedback obtained from the proposed scheme is not suffering from the force discontinuities at the edges of the mesh triangles, on contrary to the approaches that generate the force feedback directly from the meshes of the colliding objects and does not produce the overounded effect of the force shading method [20]. Moreover, simple operation like smoothing on the distance map can result to even more smooth force feedback.

► Figure 14. *(Continued)*

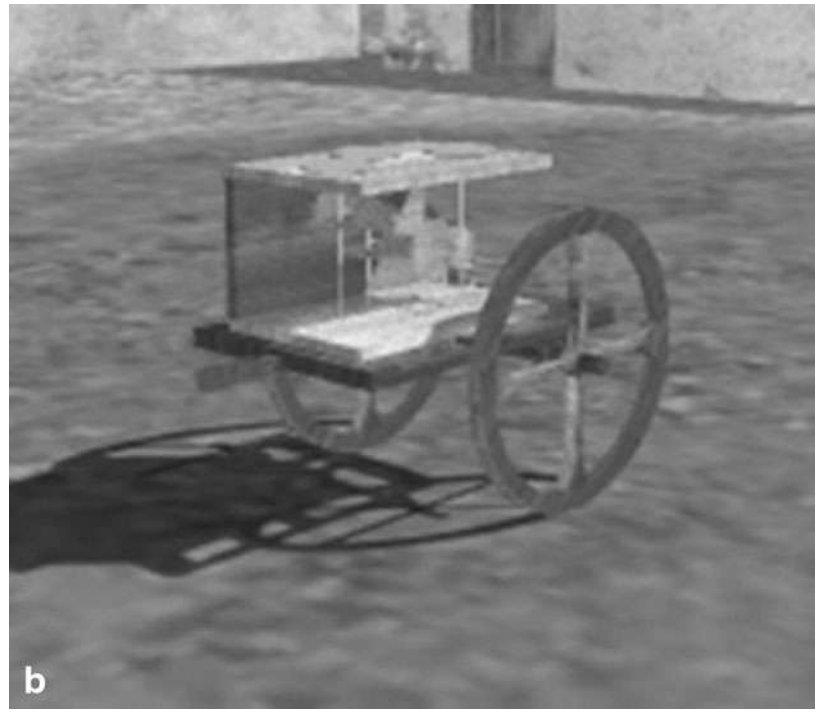

6. Evaluation

The evaluation was designed in order to help the qualitative/quantitative estimation of:

- The overall usability of the proposed technologies to nonspecialized individuals.
- The extensibility and expansibility of the use of the proposed technologies into other application fields.
- The acceptance of the tools, the user-friendliness and the points where improvement is needed.
- The performance in terms of understanding and handling the hardware.
- The added value produced by the introduction of new interaction techniques in the educational/entertainment procedure of Ancient Technologies simulation.
- The acceptance of the demonstration of the novel interaction technologies by the users.
- The educational value of the applications.

The system has been evaluated in tests with visitors of the Science Center and Technology Museum of Thessaloniki, in Greece (Figure 17).
The test procedure consisted of two phases: In the first phase, the users were introduced to the system and they were asked to use it. During this phase, the users were asked to fill a pre-test questionnaire. The questionnaire contained questions that focused on usability issues and on

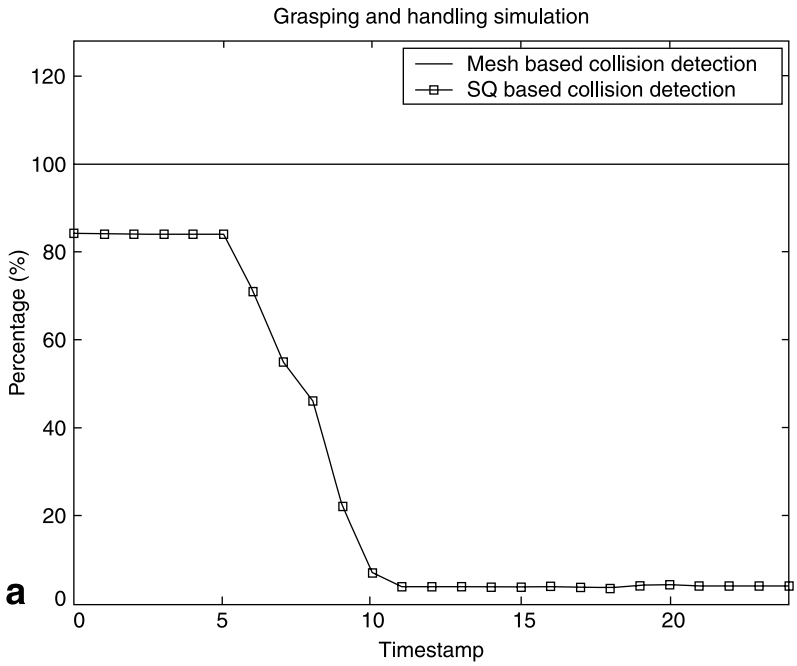

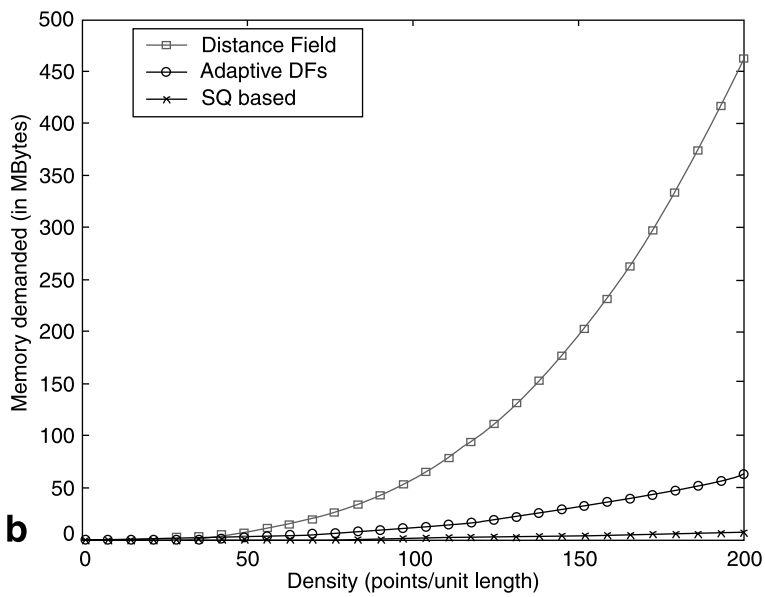

► Figure 15: a: Percentage of computational time needed to perform collision detection with the proposed method with respect to standard mesh based approaches. b: Memory requirements for the distance field, the adaptive distance field and the superquadric based method for a scene consisting of 8108 triangles.

their interest in participating to each test. The second phase was carried out immediately after the tests, using an after tests questionnaire. Specifically, the users where questioned, after finishing all the tests, about general issues such as: (a) the benefits and limitations that they foresee on this technology,

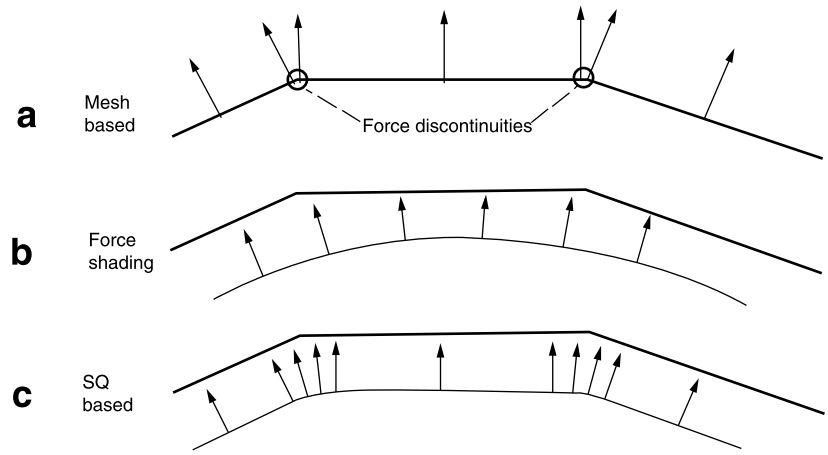

◀ Figure 16: Force feedback using (a) only the mesh, (b) force shading and (c) smoothing on the SQ distance map.

(b) the usability of the system in a museum environment, (c) other tests and applications or technologies that they would like to experiment with the application, if any, etc. The questionnaire contained also questions to the test observers, e.g. if the user performed the task correctly, how long did it take him/her to perform the task, etc.

The system evaluation results have shown that users consider it very innovative and satisfactory in terms of providing a presentation environment in a real museum. The percentage of the satisfied students was reported to be more than 95%.

7. Conclusion

In this paper a novel framework for the simulation of ancient technology works was presented. Novel virtual reality technologies for object modeling, collision detection and haptic rendering have been proposed that provide realistic interactive simulation using haptic devices. Moreover, a number of simulation scenarios have been developed and evaluated by visitors of the science center and technology museum in Thessaloniki, Greece. Specifically, the analysis of the basic characteristics of Ancient Greek Technologies are presented using virtual reality environments, so that they can become easily perceptible even in those that are not familiar with the technology. In this way, the platform contributes substantially in the general effort to promote the knowledge on Ancient Technologies.

Acknowledgements

This work was supported by the research project (PENED) that is co-financed by E.U.-European Social Fund (75%) and the Greek Ministry of Development-GSRT (25%), the research project VR@Theater and the EU funded IST Similar Network of Excellence.

► Figure 17: Users practicing the scenarios.

References

1. Iliadis, N., *Learning Technology Through the Internet.* Kastaniotis Publisher, Athens, 2002.
2. Maley, D., *The Industrial Arts teachers handbook: Techniques, principles and methods.* Allyn and Bacon, Boston, 1978.

3. Maley, D., *The Maryland plan. In American Council on Industrial Arts Teacher Education, Industrial Arts education: Retrospect, prospect.* Bloomington, Illinois, McKnight, 1979.
4. Ledermann, F., Schmalstieg, D., *Presenting an archaeological site in the virtual showcase:* Proceedings of the 2003 conference on Virtual reality, archeology, and cultural heritage, ACM Press, 2003.
5. Papaioannou, G., Christopoulos, D., *Enhancing virtual reality walkthroughs of archaeological sites.* In Proceedings of the 2003 conference on Virtual reality, archeology, and cultural heritage, ACM Press, 2003.
6. Barbieri, T., Paolini, P., *Reconstructing leonardo's ideal city—from handwritten codexes to webtalk-ii: a 3d collaborative virtual environment system.* In Proceedings of the 2001 conference on Virtual reality, archeology, and cultural heritage, ACM Press, 61–66, 2001.
7. Sparacino, F., Davenport, G., Pentland, A., *Media in performance: Interactive spaces for dance, theater, circus and museus exhibits*. IBM Systems Journal, 39(3), 479–510, 2000.
8. Tzovaras, D., Nikolakis, G., Fergadis, G., Malasiotis, S., Stavrakis, M., *Design and implementation of haptic virtual environments for the training of visually impaired.* IEEE Trans. on Neural Systems and Rehabilitation Engineering 12(2), 266–278, June 2004.
9. Nikolakis, G., Fergadis, G., Tzovaras, D., *Virtual assembly based on stereo-vision and haptic force feedback virtual reality.* In Proc. HCI International, June 2003.
10. Nikolakis, G., Fergadis, G., Tzovaras, D., Strintzis, M.G., *A mixed reality learning environment for geometry education.* In in Lecture Notes in Artificial Intelligence, Springer Verlag, June 2004.
11. Gottschalk, S., Lin, M.C., Manocha, D., *OBBTree: A Hierarchical Structure for Rapid Interference Detection,* Computer Graphics, Proc. ACM SIGGRAPH, 171–180, 1996.
12. Klosowski, J.T., M. Held, J.S.B. Mitchell, H. Sowizral, and K. Zikan, "Efficient Collision Detection Using Bounding Volume Hierarchies of k-DOPs," IEEE Trans. Visualization and Computer Graphics, 4(1), 21–36, Jan.-Mar. 1998.
13. Fuhrmann, A., Sobottka, G., Gross, C., *Distance Fields for Rapid Collision Detection in Physically Based Modeling,* In proceedings of GraphiCon '03, 58-65, September, 2003.
14. McNeely, W.A., Puterbaugh, K.D., Troy, J.J., *Six Degree-of-Freedom Haptic Rendering Using Voxel Sampling,* Computer Graphics and Interactive Techniques, 401–408, 1999.
15. Moustakas, K., Tzovaras, D., Strintzis, M.G., *SQ-Map: Efficient Layered Collision Detection and Haptic Rendering,* IEEE Transactions on Visualization and Computer Graphics, 13(1), 80–93, January 2007.
16. Solina, F., Bajcsy, R., *Recovery of parametric models from range images: The case for uperquadrics with global deformations*. IEEE Transactions on Pattern Analysis and Machine Intelligence, 12(2), 131–147, 1990.
17. Nikolakis, G., Moustakas, K., Tzovaras, D., Harissis, T., *Interactive Simulation of ancient technology works,* 5th international symposium on Virtual Reality, Archaeology and Cultural Heritage, Nicosia 2006.
18. Lin, H.S., Liao, H.M., Lin, J., *Visual salience-guided mesh decomposition.* In Proceedings of the IEEE International Workshop on Multimedia Signal Processing, 2004.
19. Frisken, S.F., Perry, R.N., Rockwood, A.P., Jones, T.R., *Adaptively Sampled Distance Fields: A General Representation of Shape for Computer Graphics,"* Computer Graphics and Interactive Techniques, 249-254, 2000.

20. Ruspini, D.C., Kolarov, K., Khatib, O., *The Haptic Display of Complex Graphical Environments,* Computer Graphics (SIGGRAPH '97 Conference Proceedings), 345-352, 1997.

Konstantinos Moustakas, Dimitrios Tzovaras
and Georgios Nikolakis
Centre for Research and Technology Hellas
Informatics and Telematics Institute
1st km Thermi-Panorama Road, P.O. Box 30361,
Thermi-Thessaloniki, Greece

{moustak, tzovaras, gniko}@iti.gr